Chinese Chemical Letters 33 (2022) 3078–3082

Contents lists available at ScienceDirect

Chinese Chemical Letters

journal homepage: www.elsevier.com/locate/cclet

AuNP aggregation-induced quantitative colorimetric aptasensing of sulfadimethoxine with a smartphone

Xiaoliang Zhang[a], Le Wang[a], Xiaochun Li[a,*], Xiujun Li[b,*]

[a] College of Biomedical Engineering, Taiyuan University of Technology, Taiyuan 030024, China
[b] Department of Chemistry and Biochemistry, University of Texas at El Paso, El Paso, Texas 79968, United States

ARTICLE INFO

Article history:
Received 4 July 2021
Revised 9 September 2021
Accepted 17 September 2021
Available online 24 September 2021

Keywords:
Smartphone
AuNP aggregation
Quantitative colorimetric assay
Antibiotics
Aptamer biosensor
Sulfadimethoxine

ABSTRACT

A gold nanoparticle (AuNP) aggregation-induced colorimetric aptasensing method for quantitative detection of sulfadimethoxine (SDM) with a smartphone was developed. AuNPs were complexed with aptamers which protected AuNPs from aggregating in high-concentration salt solutions. In the presence of SDM, SDM bound with the aptamer on the surface of AuNPs with higher affinity, which competitively desorbed the aptamer from the AuNP surface and resulted in AuNPs aggregation, accompanied with a color change from red to purple-blue. The R, G and B values of images taken by a smartphone camera were analyzed with an app on the smartphone, and were utilized for quantitative analysis of SDM. Under the optimized conditions, the colorimetric aptasensing method using a smartphone showed high sensitivity for SDM, with the limit of detection of 0.023 ppm, lower than the allowed maximum SDM residue limit. This study provides a simple, fast, and easy to read method for on-site quantitative biochemical and cellular analysis.

Antibiotics are widely used for treatment of human and animal diseases caused by pathogenic microorganisms and have played an important role in protecting human health and treatment of diseases. For instance, sulfonamides (*e.g.*, sulfadimethoxine, SDM) are a class of antibiotics that are broadly effective antibacterials to treat bacterial infections in human and animals. However, uncontrolled and incorrect use of sulfonamides antibiotics can lead to residues in food and environment, resulting in serious threats to human health [1]. The European Commission and China have adopted a maximum SDM residue limit of 100 ng/mL (~0.1 ppm) in foodstuffs of animal origin [2–5]. For accurate and sensitive detection of SDM residues in food, a variety of methods have been developed for the detection of SDM antibiotics, including high-performance liquid chromatography (HPLC) [6–8], capillary electrophoresis (CE) [9], enzyme-linked immunosorbent assay (ELISA) [10,11] and surface plasmon resonance (SPR) [12]. However, these methods are complicated and time-consuming, and require expensive equipment or highly trained personnel. Simple and rapid methods for on-site quantitative detection of sulfonamide antibiotics with high sensitivity and specificity are greatly needed.

Aptamers are DNA- or RNA-based oligonucleotide segments used for binding to various targets such as small ions, antibiotics, proteins, and cells with high affinity and specificity [13,14]. Compared with antibodies used in immunosorbent methods, aptamers are easy to synthesize, modify, and can be preserved for long a term. Aptamers have been successfully used as excellent recognition probes in various bioanalytical applications such as molecular dynamics [15,16] and diseases diagnosis [17–20]. Apatmers specific to SDM were reported [21], and have been successfully applied to the detection of SDM, combined with photoelectrochemical and colorimetric detection methods [5,22–24]. However, bulky and costly equipment is still required for the quantitative aptasensing of SDM.

Gold nanoparticles (AuNPs) have been widely used in bioassays as carriers or signal reporters owing to their unique physicochemical properties such as UV-vis absorption, fluorescence, impedance and excellent biocompatibility. In particular, the aggregation of AuNPs [25] and the corresponding change in UV-vis absorption spectra have enabled extensive applications in the detection of enzyme activity [26], nucleic acids [27], ions [28] and other biomolecules [29]. Due to high simplicity, cost-effectiveness, and detection of its colorimetric signals with the naked eye [30–34], aptamer-functionalized AuNP biosensors were developed for the colorimetric detection of SDM [5,22]. However, the UV-vis spectroscopic quantitative detection still relies on a spectrophotometer [5,22], which limits its application for on-site detection.

Owing to the powerful imaging function of modern smartphone cameras, smartphone-based analytical techniques have also

* Corresponding authors.
E-mail addresses: lixiaochun@tyut.edu.cn (X. Li), xli4@utep.edu (X. Li).

https://doi.org/10.1016/j.cclet.2021.09.061
1001-8417/

attracted increasing attention [35–38]. For example, Hong and Chang reported a smartphone app that digitizes the color of a colorimetric sensor array for the semi-quantitative detection of multiple biomarkers in urine based on their difference colors under the indoor fluorescent light and the outside sunlight [35]. Lopez-Ruiz *et al.* reported the smartphone-based simultaneous pH and nitrite colorimetric determination based on the H (hue) and S (saturation) coordinates of HSV colors in the presence of corresponding color indicators on paper-based microfluidic devices [36]. Current smartphone-based colorimetric assays mostly target intrinsic colors of analytes or simple color reactions after the addition of color indicators such as pH indicators. Combined with nucleic acid probe and AuNPs, Xu *et al.* developed a smartphone-based on-site nucleic acid testing platform in point-of-care settings [38].

In this work, we developed a new smartphone-based colorimetric aptasensing method based on AuNP aggregation for simple but quantitative detection of SDM. In the presence of SDM, the aptamer bond with the target SDM, and the aptamers were desorbed from the surface of AuNPs. As a result, the AuNPs were aggregated in high salt media, with a concomitant red-to-blue color change. The R, G and B value of images taken by a smartphone camera were analyzed by an app for quantitative bioanalysis, the R value showed good linear relationship with the concentrations of SDM, with the limit of detection (LOD) of 0.023 ppm, which was lower than the maximum SDM residue limit (~0.1 ppm) allowed by the European Commission and China. However, in the absence of SDM, no AuNP aggregation as well as color changes occurred. This smartphone-based colorimetric aptasensing method enables simple, direct, and quantitative detection of antibiotics, without using costly and bulky equipment, especially for resource-limited settings such as on-site and field detection.

The smartphone-based colorimetric aptasensing method for quantitative detection of SDM is based on the target-triggered AuNP aggregation, while using the SDM-specific aptamer as the recognition element, and analyzed R, G, or B values from captured images for quantitative analysis. Fig. 1 shows the principle of the smartphone-based colorimetric aptasensing method. As illustrated in Fig. 1a, in the absence of SDM, the aggregation of AuNPs can be induced by high-concentration salt. However, when adding the aptamer, the aptamer can be easily adsorbed on the surface of AuNPs by the electrostatic interaction between the bases of ssDNA of aptamer and AuNPs, which prevents the strong van der Waals attraction and enhances the stability of AuNPs. Thus, no AuNP aggregation happens, the color of AuNPs still remains red and the absorption wavelength maximum stays at 522 nm in the UV-vis spectra. Upon the addition of SDM, the aptamer binds to SDM with higher affinity, which induces the adsorbed aptamers to be detached from AuNPs and leads to the aggregation of AuNPs. During this process, the color changes from red to purple-blue. As shown in Fig. 1b, a smartphone is arranged to capture images and analyze their R, G or B values to determine the concentration of SDM. The transmission electron microscopy (TEM) images in Fig. 1c show the morphology changes of AuNPs before and after the aggregation.

AuNPs were prepared by citrate reduction of $HAuCl_4$. The AuNPs were prepared at room temperature by adding 1.0 mL of a 1% sodium citrate solution to 0.01% of 100 mL $HAuCl_4$ with vigorous stirring. After 1 min, 1.0 mL 0.075% of $NaBH_4$ (dissolved in 1% sodium citrate solution) was added. The mixture was not stopped from stirring until its color turned red. The average diameter of AuNPs showed by TEM was about 10 nm (Fig. 1c). The concentration of the AuNPs was about 1.3 nmol/L, which was determined according to Beer's law by using the extinction coefficient of 6.15×10^7 L mol^{-1} cm^{-1} for 10 nm AuNPs in diameter at 450 nm [39]. The prepared dispersed AuNPs solution was very stable for several months.

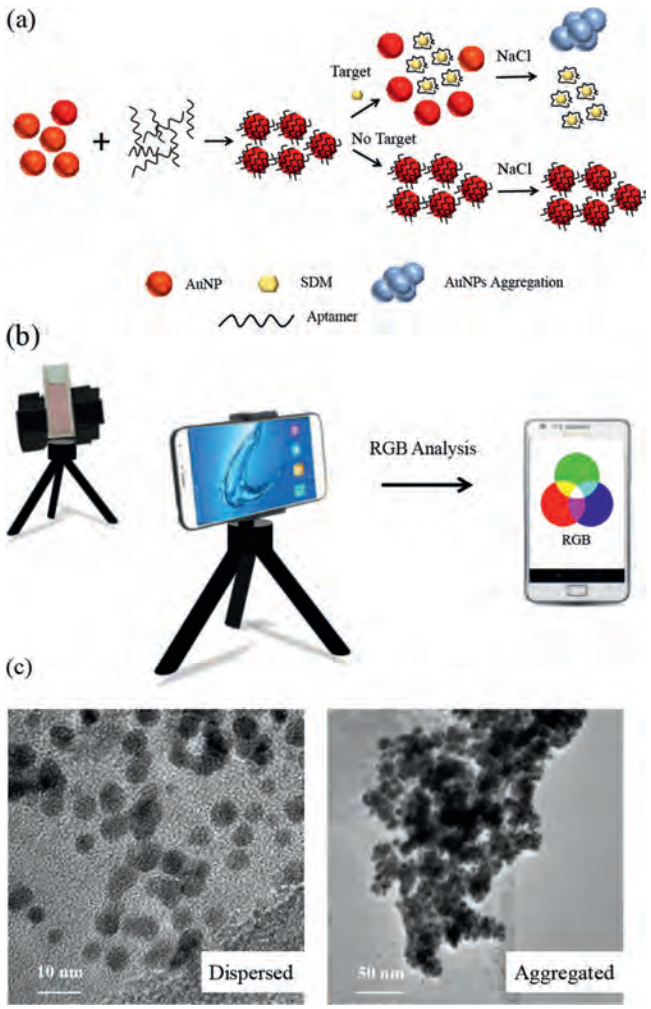

Fig. 1. Principle (a) and setup (b) of quantitative colorimetric detection of SDM based on AuNP aggregation with a smartphone. (c) TEM images of dispersed AuNPs and aggregated AuNPs induced by the target in high-concentration of NaCl solutions (0.04 mol/L).

Prior to the colorimetric aptasensing of the target, the effects of several key factors were investigated and optimized, including the concentration of NaCl and the concentration of the aptamer. AuNPs can aggregate in high-concentration NaCl solutions and the concentrations of NaCl solutions influence the degree of aggregation. Therefore, the salt concentration (NaCl) is particularly important and firstly investigated. The spectra changes of the mixture after adding different concentrations of NaCl were shown in Fig. 2a. Since high-concentration NaCl can induce the aggregation of AuNPs and the aggregated AuNPs show weaker absorbance at 522 nm compared with the dispersed AuNPs, with the increase of the NaCl concentrations, the absorption peak at 522 nm, a presentative peak for dispersed AuNPs, kept decreasing. As shown in Fig. 2b, when the NaCl concentration was greater than 0.04 mol/L, the absorbance at 522 nm did not change significantly, which indicates that almost all of AuNPs were aggregated. Therefore, 0.04 mol/L of NaCl was determined as the optimal salt concentration in our assay system.

Since SDM competes with AuNPs for binding to aptamers, the concentration of the aptamer affects the aggregation of AuNPs. If the aptamer concentration is too high, when NaCl is added to the solution, less aggregation of AuNPs will be observed, and this will affect the detection of SDM. Hence, the aptamer concentration was

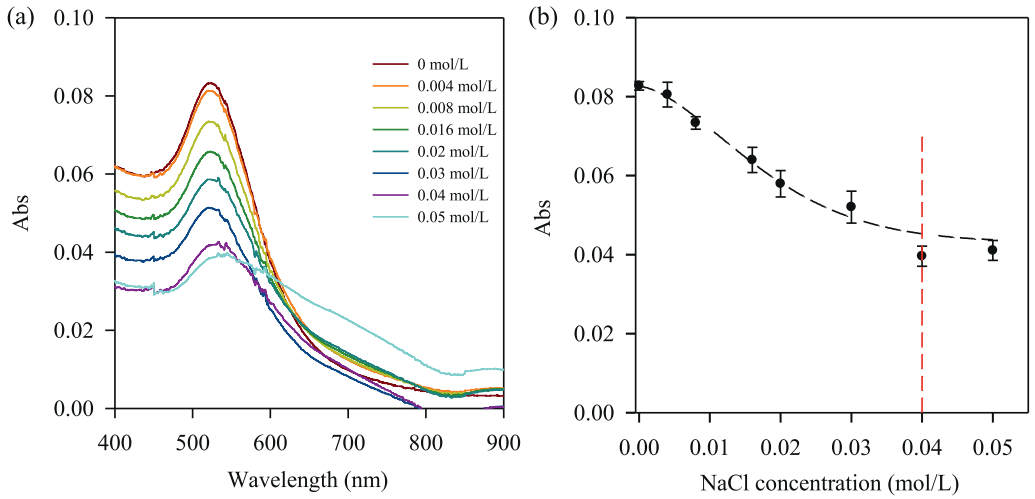

Fig. 2. The effect of different concentrations of NaCl on AuNPs aggregation. (a) The absorbance spectra of AuNPs solutions in different concentrations of NaCl. (b) UV-vis absorbance of AuNPs at 522 nm with different concentrations of NaCl.

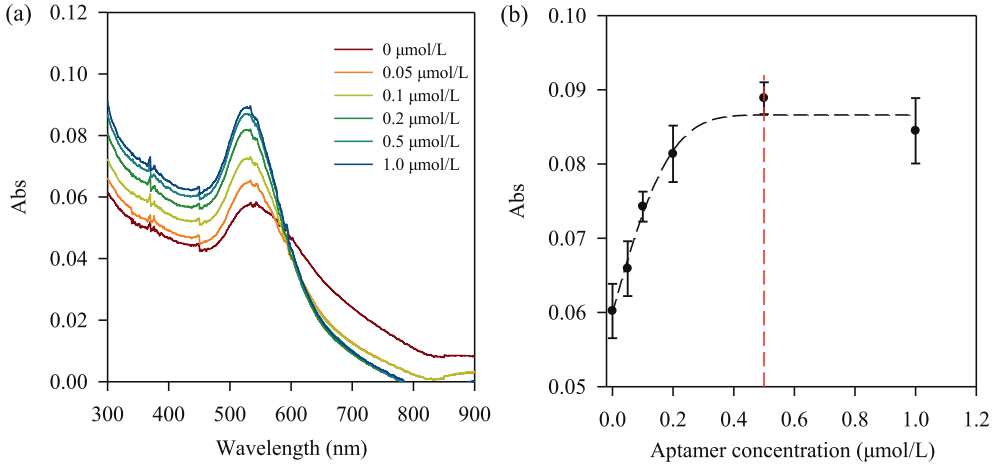

Fig. 3. Optimization of aptamer concentrations. (a) The absorbance spectra of AuNPs solutions at various concentrations of the aptamer. (b) UV-vis absorbance of AuNP solutions at 522 nm along with the changes of aptamer concentrations. NaCl concentration, 0.04 mol/L.

also optimized. The spectra changes of the mixture with different concentrations of the aptamer is shown in Fig. 3.

The absorbance at 522 nm increased with the increased concentrations of the aptamer over the range from 0 to 1.0 μmol/L, which indicates that the aptamer was adsorbed to the AuNPs surface and inhibited the aggregation of AuNPs. However, the absorbance plateaued when the concentration of the aptamer was higher than 0.5 μmol/L. Thus, 0.5 μmol/L aptamer was determined as the optimal aptamer concentration.

After condition optimization, different concentrations of the target SDM were mixed with the AuNP/aptamer solutions and measured using the AuNPs-aggregation based colorimetric aptasensing method with a smartphone. Compared with AuNPs, SDM possesses a higher affinity to the aptamer. Therefore, the presence of the SDM can desorb the aptamer from AuNPs, which further leads to the aggregation of the AuNPs in the presence of high-concentration NaCl. As shown in images taken by a smartphone camera in Fig. 4a, after the addition of SDM, an obvious color change from red to purple blue was observed with the increase of the concentration of SDM from 0 to 5 ppm.

The R, G, B values of these images were further analyzed by a smartphone app and the relationships between the R, G, B value and the concentration of SDM were investigated. Fig. S1 (Supporting information) shows that the R values decreased with the increasing concentrations of SDM in the concentration range of 0–1.0 ppm. When the concentration of SDM was higher than 1.0 ppm, the R values increased slightly and then became plateaued. Since the solution shows a color change from red to purple-blue, this nonmonotonic variation of R value can be attributed to the hue change of the solution. G and B values show a similar relationship with the concentrations of SDM. As shown in Fig. 4b, linear relationships were derived between the R, G and B values and the concentrations of SDM in the range of 0–0.6 ppm, respectively. The linear regression equations for R, G, and B curves are $y = -121.26C + 139.75$, $y = -102.90C + 112.55$, and $y = -100.01C + 150.49$, where C represents the concentration of SDM (ppm), y represents R, G and B values, respectively. Their corresponding squared correlation coefficients (R^2) are 0.9921, 0.9791, and 0.9963, respectively. The R *vs.* C curve exhibits the largest slope of the fitted lines, indicating the highest sensitivity among R, G, and B. Therefore, the R value was utilized to quantify the concentration of SDM. In addition, the limit of detection (LOD) was calculated to be 0.023 ppm based on the 3σ method, which is lower than maximum residue limit of ~0.1 ppm in foodstuffs of animal origin. The comparison of the LOD of SDM in this study with other methods is summarized in Table S1 (Supporting information). It can be seen that although our method provides a higher LOD than that from some costly instruments, it has a comparable

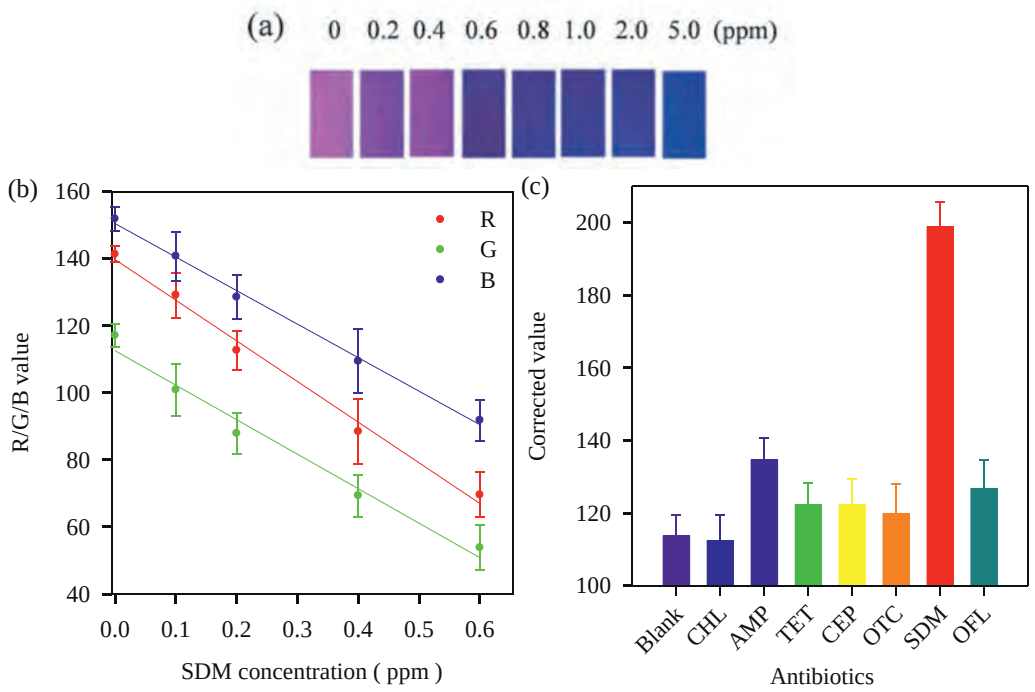

Fig. 4. (a) Images of the assay solutions taken by a smartphone camera with different concentrations of SDM. (b) The linear correlation between R, G and B values and SDM concentrations from 0 to 0.6 ppm, respectively. (c) Specificity investigation of the colorimetric aptasensing method, compared to various antibiotics (3.5 μmol/L), including chloramphenicol (CHL), ampicillin (AMP), tetracycline (TET), cephradine (CEP), oxcytetracycline dehydrate (OTC), ofloxacin (OFL), sulfadimethoxine (SDM), and Blank. For a better presentation (*i.e.*, positive peaks for the target, relative to other antibiotics), the corrected R value that is defined as 255 minus the R value of different antibiotics assay solutions was used in (c).

or even lower LOD than other label-free aptasensor methods even using spectrophotometers. Since this smartphone-based quantitative aptasensing method does not require conventional costly instruments, and thus provides a simple, fast, and easy to read method for on-site SDM analysis with high sensitivity.

The specificity of the method was also investigated. 100 μL of various concentrations of other antibiotics (3.5 μmol/L) were added to the above AuNPs/aptamer solutions and measured using the colorimetric aptasensing method, following the same protocol for the measurement of SDM. As shown in Fig. 4c, only SDM resulted in significant changes in corrected R values, and no noticeable color changes were observed in all other antibiotic solutions. Furthermore, their UV-vis spectra were recorded and shown in Fig. S2 (Supporting information). Similarly, only SDM led to a significant wavelength shift, an indication of different status of AuNPs from the dispersed status to aggregated status, while all other antibiotics only resulted in negligible changes in wavelength shift, further confirming the high specificity of our method.

In summary, we developed a smartphone-based colorimetric aptasensing method based on AuNP aggregation for quantitative detection of SDM at the point of care. Aptamer-AuNPs were used to combine the high selectivity and affinity of aptamers and the spectroscopic advantages of AuNPs to allow for simple, rapid and sensitive detection of SDM. The red-to-blue color change of AuNPs in the presence of SDM was captured by a smartphone camera and the R Value was digitalized for quantitative detection of SDM. The LOD was calculated to be 0.023 ppm, lower than the maximum SDM residue limit. This colorimetric aptasensing method provides a powerful tool for on-site screening of antibiotic residues. By changing different aptamers [40–42] and combining with microfluidic platforms [43–45], this smartphone-based colorimetric method has great potential for simple and quantitative biochemical and cellular analysis at various low-resource settings such as on-site detection [46–50].

Supplementary material

Supplementary material related to this article such as more detailed experimental sections can be found, in the online version at

Declaration of competing interest

A China Patent (ZL 201710957744.6) was granted on December 22, 2020 for which the inventors are Xiaochun Li, Le Wang, Xiaoliang Zhang and Hua-Zhong Yu. The patent covers the method of AuNPs aggregation-based quantitative colorimetric aptasensing of sulfadimethoxine with a smartphone described herein. The inventors have begun dialogues with a number of biotech companies to explore its commercialization.

Acknowledgments

This work was supported by the National Natural Science Foundation of China (Nos. 21874098 and 61775157), and Program for the Outstanding Innovative Teams of Higher Learning Institutions of Shanxi, Key R&D plan of Shanxi Province (International cooperation) (No. 201903D421053), Key R&D Plan of Shanxi Province (high technologies field, No. 201903D121158), and the U.S. NSF (Nos. IIP2122712 and IIP 2052347), CPRIT (No. RP210165), and DOT (No. CARTEEH).

Supplementary materials

Supplementary material associated with this article can be found, in the online version, at doi:10.1016/j.cclet.2021.09.061.

References

[1] A. Białk-Bielińska, J. Maszkowska, W. Mrozik, A. Bielawska, et al., Chemosphere 86 (2012) 1059–1065.

[2] European Economic Community, Off. J. Eur. Community L60 (1999) 16–52.
[3] Animal Husbandry and Veterinary Bureau of Ministry of Agriculture, Chin. J. Vet. Drug 37 (2003) 15–20.
[4] X.L. Wang, K. Li, D.S. Shi, et al., J. Agric. Food Chem. 55 (2007) 2072–2078.
[5] A.L. Chen, X.L. Jiang, W.W. Zhang, et al., Biosens. Bioelectron. 42 (2013) 419–425.
[6] W.M.M. Mahmoud, N.D. H.Khaleel, G.M. Hadad, et al., Clean Soil Air Water 41 (2013) 907–916.
[7] M. Seifrtova, L. Novakova, C. Lino, et al., Anal. Chim. Acta 649 (2009) 158–179.
[8] N.T. Malintan, M.A. Mohd, J. Chromatogr. A 1127 (2006) 154–160.
[9] R. Hoff, T.B.L. Kist, J. Sep. Sci. 32 (2009) 854–866.
[10] M.T. Muldoon, S.A. Buckley, S.S. Deshpande, et al., J. Agric. Food Chem. 48 (2000) 545–550.
[11] I. S.Nesterenko, M.A. l. Noke, S.A. Eremin, J. Anal. Chem. 64 (2009) 435–444.
[12] T. Mcgrath, A. Baxter, J. Ferguson, S. Haughey, P. Bjurling, Anal. Chim. Acta 529 (2005) 123–127.
[13] K. Sefah, D. Shangguan, X.L. Xiong, M.B. O'Donoghue, W.H. Tan, Nat. Protoc. 5 (2010) 1169–1185.
[14] P. Zuo, X. Li, D.C. Dominguez, B.C. Ye, Lab Chip 13 (2013) 3921–3928.
[15] M. Berezovski, R. Nutiu, Y.F. Li, S.N. Krylov, Anal. Chem. 75 (2003) 1382–1386.
[16] K.L. Rhinehardt, G. Srinivas, R.V. Mohan, J. Phys. Chem. B 119 (2015) 6571–6583.
[17] X.H. Fang, W.H. Tan, Acc. Chem. Res. 43 (2010) 48–57.
[18] W. Sheng, T. Chen, W.H. Tan, Z.H. Fan, ACS Nano 7 (2013) 7067–7076.
[19] X. Wu, J. Chen, M. Wu, X.J. Zhao, Theranostics 5 (2015) 322–344.
[20] A.B. Iliuk, L.H. Hu, W.A. Tao, Anal. Chem. 83 (2011) 4440–4452.
[21] K. Song, E. Jeong, W. Jeon, H. Jo, C. Ban, Biosens. Bioelectron. 33 (2012) 113–119.
[22] S. C.Niu, Z.Z. Lv, J.C. Liu, et al., Plos One 9 (2014) e109263.
[23] O.K. Okoth, K. Yan, Y. Liu, J.D. Zhang, et al., Biosens. Bioelectron. 86 (2016) 636–642.
[24] A.C. Wang, H.M. Zhao, X.C. Chen, et al., Anal. Biochem. 525 (2017) 92–99.
[25] J.W. Liu, Y. Lu, Nat. Protoc. 1 (2006) 246–252.
[26] S. Li, L.Y. Mao, Y.P. Tian, J. Wang, N. Zhou, Analyst 137 (2012) 823–825.
[27] W. Zhou, K. Hu, S. Kwee, et al., Anal. Chem. 92 (2020) 2739–2747.
[28] G. G.Huang, Y.T. Chen, Y.R. Lin, Anal. Methods 6 (2014) 5690–5696.
[29] J. Dapra, L.H. Lauridsen, A.T. Nielsen, N. Rozlosnik, Biosens. Bioelectron. 43 (2016) 315–320.
[30] F. Pena-Pereira, I. Lavilla, C. Bendicho, Sens. Actuators B 242 (2017) 940–948.
[31] Y. Jiang, M.L. Shi, Y. Liu, et al., Angew. Chem. Int. Ed. 56 (2017) 11916–11920.
[32] C.Y. Lin, C.J. Yu, Y.H. Lin, W.L. Tseng, Anal. Chem. 82 (2010) 6830–6837.
[33] C.S. Wang, J. Liu, X.Y. Han, et al., Anal. Methods 9 (2017) 4843–4850.
[34] M.L. Zhou, T. Lin, X.X. Gan, Microchim. Acta 184 (2017) 4671–4677.
[35] J.I. Hong, B.Y. Chang, Lab Chip 14 (2014) 1725–1732.
[36] N. Lopez-Ruiz, V.F. Curto, M.M. Erenas, et al., Anal. Chem. 86 (2014) 9554–9562.
[37] X. Xu, A. Akay, H. Wei, et al., Proc. IEEE 103 (2015) 236–247.
[38] X. Xu, X. Wang, J. Hu, et al., Electrophoresis 40 (2019) 914–921.
[39] W. Haiss, J. Aveyard, D.G. Fernig, Anal. Chem. 79 (2007) 4215–4221.
[40] W. Zhou, K. Hu, S. Kwee, et al., Anal. Chem. 92 (2020) 2739–2747.
[41] M. Dou, J.M. Garcia, S. Zhan, X. Li, Chem. Comm. 52 (2016) 3470–3473.
[42] M. Lv, W. Zhou, H. Tavakoli, et al., Biosens. Bioelectron. 176 (2021) 112947.
[43] W. Zhou, M. Dou, S.T. Sanjay, F. Xu, X. Li, Lab Chip 21 (2021) 2658–2683.
[44] X.J. Li, Z.H. Nie, C.M. Cheng, A.B. Goodale, G.M. Whitesides, Proc. Micro Total Anal. Syst. 14 (2010) 1487–1489.
[45] M. Dou, N. Macias, F. Shen, et al., eClinicalMedicine 8 (2019) 72–77.
[46] H. Tavakoli, W. Zhou, L. Ma, et al., TrAC Trends Anal. Chem. 117 (2019) 13–26.
[47] S.T. Sanjay, G. Fu, M. Dou, et al., Analyst 140 (2015) 7062–7081.
[48] X.J. Li, A.V. Valadez, P. Zuo, Z. Nie, Bioanalysis 4 (2012) 1509–1525.
[49] J. Zhang, X. Wei, R. Zeng, F. Xu, X. Li, Future Sci. OA 3 (2017) FSO187.
[50] S.T. Sanjay, W. Zhou, M. Dou, et al., Adv. Drug Deliv. Rev. 128 (2018) 3–28.